



Cyclic diarylheptanoids as Na⁺-glucose cotransporter (SGLT) inhibitors from *Acer nikoense*

Hiroshi Morita^{a,*}, Jun Deguchi^a, Yusuke Motegi^a, Seizo Sato^b, Chihiro Aoyama^b, Jiro Takeo^b, Motoo Shiro^c, Yusuke Hirasawa^a

^a Faculty of Pharmaceutical Sciences, Hoshi University, Ebara 2-4-41 Shinagawa-ku, Tokyo 142-8501, Japan

^b Central Research Laboratory, Nippon Suisan Kaisha, Ltd, 559-6 Kitano-machi, Hachioji, Tokyo 192-0906, Japan

^c X-ray Research Laboratory, Rigaku Corporation, Akishima, Tokyo 196-8666, Japan

ARTICLE INFO

Article history:

Received 13 October 2009

Revised 14 November 2009

Accepted 7 December 2009

Available online 11 December 2009

Keywords:

Acerogenin

Acer nikoense

SGLT inhibitor

Conformational analysis

ABSTRACT

Two cyclic diarylheptanoids, acerogenins A (**1**) and B (**2**) have been isolated from the bark of *Acer nikoense* as inhibitors of Na⁺-glucose cotransporter (SGLT). Acerogenins A (**1**) and B (**2**) inhibited both isoforms, SGLT1 and SGLT2. Structure–activity relationship of acerogenin derivatives on inhibitory activity of SGLT as well as conformational analysis of **1** and **2** on the basis of *J*-resolved HMBC spectra and X-ray analysis were discussed.

© 2009 Elsevier Ltd. All rights reserved.

Na⁺-glucose cotransporter (SGLT) is a membrane protein that plays an important role in the re-absorption of glucose in the kidneys. SGLT is known to have three isoforms (SGLT1, SGLT2, and SGLT3).^{1–3} SGLT1 is expressed primarily in the brush border membrane of mature enterocytes in the small intestine, where it absorbs dietary glucose and galactose from the gut lumen.⁴ SGLT2 is only expressed in the renal cortex, where it is assumed to be present in the brush border membrane of the S1 and S2 segments of the proximal tubule, and to be responsible for the re-absorption of glucose from the glomerular filtrate.⁴ It is expected that the inhibition of SGLT could decrease glucose re-absorption resulting in an increase in urinary sugar excretion and a decrease in blood glucose level. Thus, SGLT inhibitors have therapeutic potential for type 2 diabetes.⁵

Our screening study on SGLT inhibitors in traditional medicines discovered that the bark of methanol extract of *Acer nikoense* showed effective SGLT inhibitory activity. The bark of *Acer nikoense* (Aceraceae) are used as a Japanese folk medicine for hepatic disorders and eye diseases, which contains a series of acerogenins^{6,7} and acerosides^{8,9} with a range of biological activities such as anti-cancer, anti-inflammatory, anti-fungal, and anti-bacterial effects.¹⁰ Our efforts on identifying inhibitors that target SGLT1 and SGLT2 resulted in the isolation of two cyclic diarylheptanoids, acerogenins A (**1**) and B (**2**) from the bark of *Acer nikoense*. Our interest

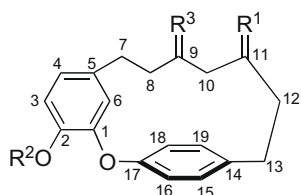
has also been focused on conformation of these cyclic diarylheptanoids with SGLT inhibition to clarify structure–activity relationship. This paper describes effects of acerogenins A (**1**) and B (**2**) on inhibition of SGLT and structure–activity relationship of these cyclic diarylheptanoids as well as conformational analysis of **1** and **2** by *J*-resolved HMBC spectra and X-ray analysis of **2**.

The bark of *Acer nikoense* (1.0 kg) was extracted with MeOH, and the extract was partitioned between hexane and water. Hexane-soluble materials (7.3 g) were subjected to a silica gel column (hexane/EtOAc), in which a bioactive fraction eluted with 10% EtOAc was purified by an ODS HPLC (70% MeOH) to afford acerogenins A⁶ (**1**, 268 mg, 0.03% yield) and B⁷ (**2**, 99 mg, 0.01% yield) as SGLT inhibitors. Then, the known related diarylheptanoids such as aceroside I (**3**)⁸ and VII (**4**)⁹ were also isolated from water soluble materials.

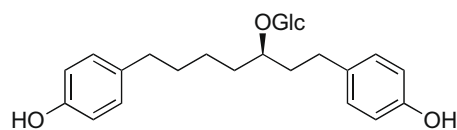
In this study, the SGLT inhibitory activities of acerogenins **1–4** and their derivatives **5–20** against [¹⁴C]methyl- α -D-glucopyranoside uptake in COS-1 cells expressing hSGLT1 or hSGLT2 were evaluated (Table 1).¹¹ It was found that acerogenins A (**1**) and B (**2**) remarkably inhibited SGLT1 [IC₅₀ (μ M) **1**: 20.0; **2**: 26.0], and weakly against SGLT2 [IC₅₀ (μ M) **1**: 94.0; **2**: 43.0]. Whereas aceroside I (**3**) with a glucose at a phenolic hydroxy group and aceroside VII (**4**), acyclic diarylheptanoid with a glucose at C-11, did not show inhibition of both SGLT1 and SGLT2. Position of a hydroxy group at C-9 or C-11 and their stereochemistry may not be so influenced for SGLT inhibition. On the other hand, some derivatives of **1** such as a methyl ether **5** and a ketone **6** (acerogenin C),¹² a ketone of a

* Corresponding author. Tel./fax: +81 354985778.

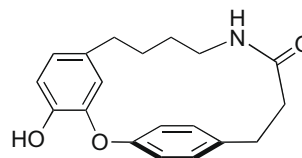
E-mail address: moritah@hoshi.ac.jp (H. Morita).



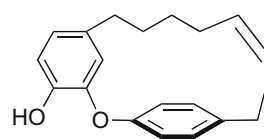
- 1** : R¹ = OH (β), H, R² = H, R³ = H₂ (acerogenin A)
2 : R¹ = H₂, R² = H, R³ = OH, H (acerogenin B)
3 : R¹ = OH (β), H, R² = Glc, R³ = H₂ (aceroside I)
5 : R¹ = OH (β), H, R² = Me, R³ = H₂
6 : R¹ = O, R² = H, R³ = H₂ (acerogenin C)
7 : R¹ = O, R² = Me, R³ = H₂
8 : R¹ = H₂, R² = Me, R³ = OH, H
9 : R¹ = H₂, R² = Me, R³ = O
10 : R¹ = OAc (β), H, R² = Ac, R³ = H₂
11 : R¹ = OBz (β), H, R² = Bz, R³ = H₂
12 : R¹ = OCOCH(CH₃)₂ (β), H, R² = COCH(CH₃)₂, R³ = H₂
13 : R¹ = OBz (*p*-Cl) (β), H, R² = Bz (*p*-Cl), R³ = H₂
14 : R¹ = OH (β), H, R² = Bn, R³ = H₂
15 : R¹ = O, R² = Ac, R³ = H₂
16 : R¹ = O, R² = Bn, R³ = H₂
17 : R¹ = O, R² = Bz, R³ = H₂
18 : R¹ = H₂, R² = H, R³ = H₂



4 (aceroside VII)



19



20

Table 1
Effects of acerogenins and their derivatives on SGLT inhibitory activity

	Inhibition ^a (%)	
	SGLT1	SGLT2
1	92.7	33.9
2	94.2	54.2
3	18.3	15.0
4	9.7	14.1
5	67.8	29.5
6	44.9	67.8
7	44.6	53.3
8	77.9	62.4
9	37.7	65.4
10	68.8	67.5
11	-1.7	-9.7
12	20.6	34.3
13	15.7	16.8
14	31.4	45.3
15	13.5	19.3
16	3.9	19.8
17	1.4	45.2
18	96.3	77.4
19	46.5	76.9
20	73.7	15.3
Phlorizin ^b	50.0	80.0

^a All compounds were evaluated at 50 μM.

^b Phlorizin was evaluated at 0.2 μM.

methyl ether **7**, and derivatives of **2** such as a methyl ether **8** and a ketone of a methyl ether **9** were prepared with diazomethane and/or Jones reagent. Treatment of acerogenin A (**1**) and **6** with appropriate acid chloride and DMAP in CHCl₃ afforded ester derivatives **10–13**, **15**, and **17**. Ether derivatives **14** and **16** were prepared from **1** by use of benzyl bromide. Dehydroxylated derivative **18** was converted from **1** and **6**, respectively, by treatment with *p*-toluene

sulfonyl chloride and Et₃N, and then LiAlH₄. Amide derivative **19** was converted from **6** by treatment with NH₂OH, followed by treatment of LiAlH₄. Dehydrated derivative **20** was prepared from **1** by treatment with *p*-TsOH. Among the ester and ether derivatives at R² (Table 1), the acetyl and methyl ether derivatives **5**, **7**, **8**, **9**, and **10** exhibited moderate inhibitory activity against SGLT1. The ketone derivatives at R¹ such as **6**, **7**, and **9** showed more potent inhibitory activity against SGLT2. Derivatives with bulky substituents such as benzoyl and benzyl at R¹ or R² showed less effective activity against both SGLT1 and SGLT2. Dehydroxylated derivative **18** showed most potent inhibition against both SGLT1 and SGLT2, indicating that the presence of a hydroxy at C-9 or C-11 may be not important for the SGLT inhibitory activity. Interestingly, amide derivative **19** with 16-membered ring system and dehydrated derivative **20** with Z double bond at C-11 showed less activity than **18**. Therefore, the ring conformation of acerogenin derivatives is important for the SGLT inhibitory activity.

Our interest of SGLT inhibition for cyclic diaryl formation led to elucidate the three-dimensional structures of acerogenins A (**1**) and B (**2**). The flexibility of cyclic molecules in solution is somewhat difficult to determine the conformation, although the NMR provides the most reliable information in solution. To elucidate the conformation of **1** and **2** in solution, complete assignments of the ¹H and ¹³C signals were made by 2D NMR measurements (Table 2).

Conformation of acerogenin A (**1**) as shown in computer generated 3D drawing (Fig. 1) was deduced from crosspeaks observed in the NOESY spectrum, and ³J_{H-H} and ³J_{H-C} coupling constants. NOESY correlations of H-13b/H-15 and H-13a/H-19 suggested that these four protons were in one plane. *J*-resolved HMBC technique enabled to detect long range C-H *J* couplings of this cyclic structure.¹³ The coupling constants, ³J_{H13a/H12b} = 3.3 Hz, ³J_{H13a/H12a} = 3.5 Hz, ³J_{H13b/H12a} = 13.2 Hz, ³J_{H13b/H12b} = 4.2 Hz, ³J_{H13a/C11} = 8.6 Hz,

Table 2
 ^1H [δ_{H} (J, Hz)] and ^{13}C NMR data (δ_{C}) of acerogenins A (**1**) and B (**2**) in CD_3OD at 300K

	δ_{H}		δ_{C}	
	1	2	1	2
1			150.5	151.5
2			145.0	145.7
3	7.20 (1H, d, 7.8)	7.22 (1H, d, 8.4)	116.9	117.8
4	6.73 (1H, dd, 7.8, 1.8)	6.77 (1H, d, 8.4)	122.2	123.2
5			132.5	133.8
6	5.95 (1H, d, 1.8)	5.96 (1H, br s)	116.5	116.7
7a	2.45 (1H, m)	2.70 (1H, ddd, 16.8, 4.8, 3.0)	31.6	29.3
7b	2.45 (1H, m)	3.03 (1H, ddd, 16.8, 10.8, 3.0)		
8a	1.29 (1H, m)	1.76 (1H, m)	28.1	37.7
8b	1.51 (1H, m)	1.67 (1H, m)		
9a	1.00 (1H, m)	3.38 (1H, m)	24.9	71.1
9b	1.25 (1H, m)			
10a	1.39 (1H, m)	0.97 (1H, ddd, 11.1, 11.1, 7.2)	39.4	40.0
10b	1.12 (1H, m)	1.47 (1H, m)		
11a	3.53 (1H, dddd, 4.2, 4.2, 4.2, 4.2)	1.17 (1H, m)	69.3	23.5
11b		1.47 (1H, m)		
12a	1.71 (1H, dddd, 13.2, 13.2, 4.5, 3.5)	1.47 (1H, m)	40.6	31.2
12b	2.13 (1H, dddd, 13.2, 4.2, 4.2, 3.3)	1.67 (1H, m)		
13a	2.94 (1H, ddd, 13.2, 3.5, 3.3)	2.64 (1H, ddd, 13.2, 6.0, 4.5)	32.3	35.7
13b	2.76 (1H, ddd, 13.2, 13.2, 4.2)	2.48 (1H, ddd, 13.2, 9.6, 4.8)		
14			139.5	139.9
15	7.24 (1H, dd, 8.4, 1.8)	7.13 (1H, dd, 8.4, 1.2)	131.5	132.5
16	7.00 (1H, dd, 8.4, 2.4)	6.93 (1H, dd, 8.4, 2.4)	122.7	124.1
17			156.3	156.9
18	7.26 (1H, dd, 8.4, 2.4)	7.25 (1H, dd, 8.4, 2.4)	123.9	123.9
19	7.31 (1H, dd, 8.4, 1.8)	7.28 (1H, dd, 8.4, 1.2)	130.0	131.3

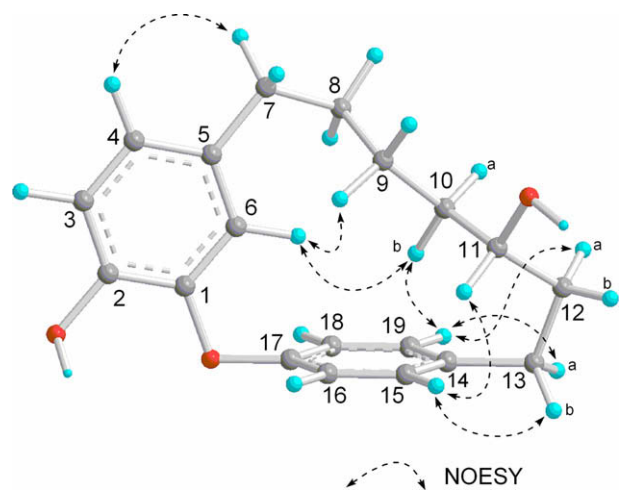
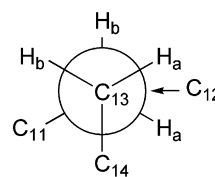


Figure 1. Selected NOESY correlations and relative stereochemistry for acerogenin A (**1**).

and $^3J_{\text{H}13\text{b}/\text{C}11} = 4.7$ Hz indicated *gauche* conformation between C-14 and C-11 (Fig. 2). Thereto, NOESY correlations of H-12a/H-19 and H-11/H-14 supported the relative stereostructure of **1**. Furthermore, NOESY correlations for H-4/H-7, H-6/H₂-9 and H-10b, and H-10b/H-19 indicated the connectivity of C-7–C-12 might be a zigzag structure as shown in Figure 1. In this conformation, the aromatic ring (C-14–C-19) is close to H-6 (δ_{H} 5.95), H-9a (δ_{H} 1.00), and H-10b (δ_{H} 1.12) and these protons are expected to be shielded by the aromatic ring. Thus, the conformation of **1** in solution was assigned as shown in Figure 1.

Acerogenin B (**2**) is a C-9 hydroxy isomer of acerogenin A (**1**). The gross structure of **2** was elucidated in a uniform manner. Conformation of **2** as shown in computer generated 3D drawing (Fig. 3) was deduced from crosspeaks observed in the NOESY spectrum and 3J coupling constants. NOESY correlations of H-13b/H-15 and H-13a/H-19 suggested that these four protons were in one plane.



$$\begin{aligned}
 {}^3J_{\text{H}13\text{a}/\text{H}12\text{b}} &= 3.3 \text{ Hz} && \textit{gauche} \\
 {}^3J_{\text{H}13\text{a}/\text{H}12\text{a}} &= 3.5 \text{ Hz} && \textit{gauche} \\
 {}^3J_{\text{H}13\text{b}/\text{H}12\text{a}} &= 13.2 \text{ Hz} && \textit{anti} \\
 {}^3J_{\text{H}13\text{b}/\text{H}12\text{b}} &= 4.2 \text{ Hz} && \textit{gauche} \\
 {}^3J_{\text{H}13\text{a}/\text{C}11} &= 8.6 \text{ Hz} && \textit{anti} \\
 {}^3J_{\text{H}13\text{b}/\text{C}11} &= 4.7 \text{ Hz} && \textit{gauche}
 \end{aligned}$$

Figure 2. Rotation model for C-11, C-12, C-13, and C-14 of **1**.

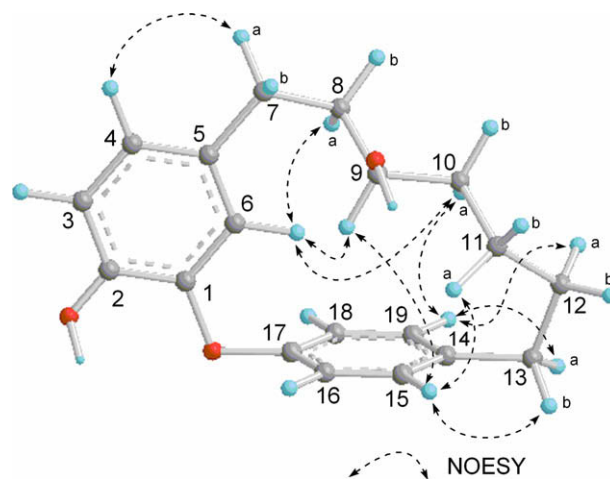


Figure 3. Selected NOESY correlations and relative stereochemistry for acerogenin B (**2**).

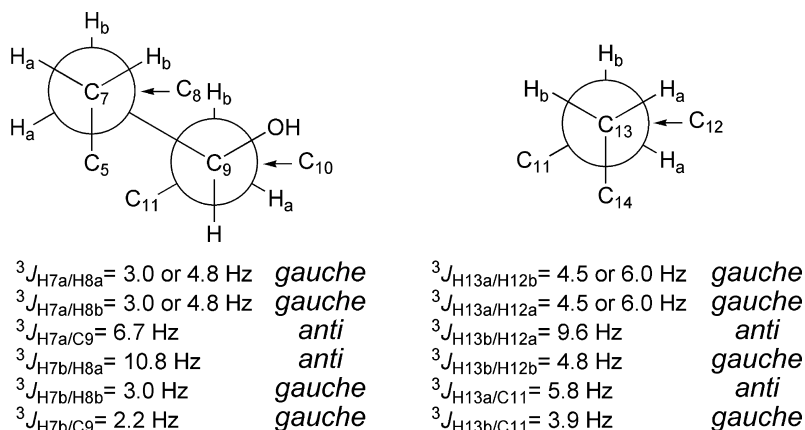


Figure 4. Rotation model for C-5, C-7, C-8, C-9, and C-10, and C-11, C-12, C-13, and C-14 of **2**.

The conformations of C-11–C-13 and C-7–C-9 were deduced from 3J coupling constants. The coupling constants, ${}^3J_{H13a/H12b} = 4.5$ or 6.0 Hz, ${}^3J_{H13a/H12a} = 4.5$ or 6.0 Hz, ${}^3J_{H13b/H12a} = 9.6$ Hz, ${}^3J_{H13b/H12b} = 4.8$ Hz, ${}^3J_{H13a/C11} = 5.8$ Hz, and ${}^3J_{H13b/C11} = 3.9$ Hz indicated *gauche* conformation between C-14 and C-11. On the other hands, the coupling constants, ${}^3J_{H7a/H8a} = 3.0$ or 4.8 Hz, ${}^3J_{H7a/H8b} = 3.0$ or 4.8 Hz, ${}^3J_{H7a/C9} = 6.7$ Hz, ${}^3J_{H7b/H8a} = 10.8$ Hz, ${}^3J_{H7b/H8b} = 3.0$ Hz, and ${}^3J_{H7b/C9} = 2.2$ Hz indicated *gauche* conformation between C-5 and C-9. NOESY correlations of H-4/H-7a, H-6/H-8a, H-6/H-9 and H-10a, and H-9/H-15 supported the relative stereostructure of **2** (Fig. 4). Thereto, NOESY correlations of H-13b/H-15, H-13a/H-19, H-12a/H-19, and H-11a/H-15 supported the relative stereostructure of **2** (Fig. 3). Furthermore, NOESY correlation for H-10a/H-19 indicated the connectivity of C-7–C-12 might be a zigzag structure. H-6 (δ_H 5.96) and H-9 (δ_H 3.38) are expected to be shielded by the aromatic ring (C-14–C-19). Thus, the conformation of **2** was assigned as shown in Figure 3. This conformational feature of **2** was also supported by Monte Carlo (MC) search.¹⁴ A total of 3000 MC steps were performed to confirm the reproducibility of calculation results. After the MC conformational search, each of the resulting conformations was subjected to the energy-minimization calculation by MMFF force field.^{15,16} Low energy conformers belonged to two separate clusters. Lowest energy one was corresponding with solution conformer (266.20 kJ/mol) analyzed by NMR in Figure 3 and the next one was solid state conformer (270.08 kJ/mol) as shown below.

Acerogenin B (**2**) was crystallized from methanol–water as colorless needles and was analyzed by X-ray crystallography.¹⁷ The asymmetric unit contains two molecules of **2**, giving a calculated density of 1.285 g cm^{-3} . The ORTEP drawing of **2** were shown in Figure 5. The configuration at C-9 in **2** obtained from X-ray analysis corresponded well to that (racemate) proposed previously.⁷ The dihedral angles of the backbone of **2** are summarized in Table 3. Each conformation of **2** in solid and solution state might be different in the dihedral angles of the cyclic side chain (C-9–C-13). The solid conformation of **2** did not take a zigzag conformation like that in solution. There were no intramolecular hydrogen bonds, which stabilized the 15-membered cyclic nature. It is a first report for X-ray structure of acerogenins. The conformation of the two aromatic rings (C-1–C-6 and C-14–C-19) is essentially twisted with extended antiparallel side chains at C-5 and C-14.

Common structural feature among acerogenins is the presence of two aromatic rings with a biphenyl ether linkage which can be connected through seven atoms bridge spacer. Orientation of the two aromatic rings is required to be ca. 125° . Conformational analysis of **1** and **2** indicated that acerogenins A and B took a similar conformation each other but did not match with that in solid state. The appropriate torsion between two aromatic planes as well as

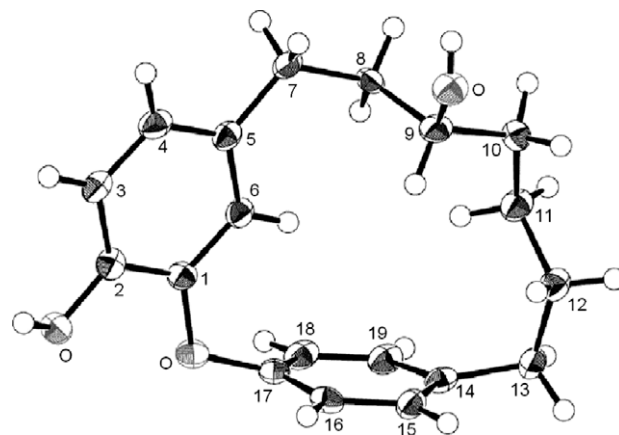


Figure 5. ORTEP Drawing for acerogenin B (**2**).

Table 3

Parts of torsion angles ($^\circ$) along backbone of acerogenin B (**2**)

	2 ^a	2 ^b
C4–C5–C7–C8	170	174.5 (2)
C5–C7–C8–C9	–70	–74.3 (3)
C7–C8–C9–C10	154	–177.0 (2)
C8–C9–C10–C11	179	–80.6 (2)
C9–C10–C11–C12	157	–96.5 (3)
C10–C11–C12–C13	–105	161.2 (3)
C11–C12–C13–C14	55	–65.3 (3)
C12–C13–C14–C15	–103	–69.0 (2)

Each angle was estimated from 3D structures based on NMR analysis, which was also supported by MC search, and on X-ray analysis.

^a Angles from molecular modeling based on NMR analysis.

^b Angles from X-ray crystallographic structure.

their conformations may be important to show inhibition of SGLT. A series of marchantins from the liverworts are similar case possessing the two aromatic rings with a biphenyl ether linkage.¹⁸ Efforts are currently underway to determine the detail structure–activity relationship for SGLT inhibitory activity of a series of acerogenins.

Acknowledgments

This work was partly supported by a Grant-in-Aid for Scientific Research from the Ministry of Education, Culture, Sports, Science,

and Technology of Japan, and a grant from the Open Research Center Project.

References and notes

1. Lee, W.-S.; Kanai, Y.; Wells, R. G.; Hediger, M. A. *J. Biol. Chem.* **1994**, *269*, 12032.
2. You, G.; Lee, W.-S.; Barros, E. J. G.; Kanai, Y.; Huo, T.-L.; Khawaja, S.; Wells, R. G.; Nigam, S. K.; Hediger, M. A. *J. Biol. Chem.* **1995**, *270*, 29365.
3. Mackenzie, B.; Panayotova-Heiermann, M.; Loo, D. D. F.; Lever, J. E.; Wright, E. M. *J. Biol. Chem.* **1994**, *269*, 22488.
4. Wright, E. M.; Turk, E. *Pflugers Arch.* **2004**, *447*, 510.
5. Katsuno, K.; Fujimori, Y.; Takemura, Y.; Hitatochi, M.; Itho, F.; Komatsu, Y.; Fujikura, H.; Isaji, M. *J. Pharm. Exp. Ther.* **2007**, *320*, 323.
6. Nagai, M.; Kubo, M.; Fujita, M.; Inoue, T.; Matsuo, M. *Chem. Commun.* **1976**, 338.
7. Kubo, M.; Inoue, T.; Nagai, M. *Chem. Pharm. Bull.* **1980**, *28*, 1300.
8. Nagai, M.; Kubo, M.; Fujita, M.; Inoue, T.; Matsuo, M. *Chem. Pharm. Bull.* **1978**, *26*, 2805.
9. Nagai, M.; Kenmochi, N.; Fujita, M.; Furukawa, N.; Inoue, T. *Chem. Pharm. Bull.* **1986**, *34*, 1056.
10. (a) Inoue, T. *Yakugaku Zasshi* **1993**, *113*, 181; (b) Ishida, J.; Kozuka, M.; Wang, H.-K.; Konoshima, T.; Tokuda, H.; Okuda, M.; Yang Mou, X.; Nishino, H.; Sakurai, N.; Lee, K.-H.; Nagai, M. *Cancer Lett.* **2000**, *159*, 135; (c) Ishida, J.; Kozuka, M.; Tokuda, H.; Nishino, H.; Nagumo, S.; Lee, K.-H.; Nagai, M. *Bioorg. Med. Chem.* **2002**, *10*, 3361; (d) Morikawa, T.; Tao, J.; Toguchida, I.; Matsuda, H.; Yoshikawa, M. *J. Nat. Prod.* **2003**, *66*, 86; (e) Akihisa, T.; Taguchi, Y.; Yasukawa, K.; Tokuda, H.; Akazawa, H.; Suzuki, T.; Kimura, Y. *Chem. Pharm. Bull.* **2006**, *54*, 735; (f) Kang, H.-M.; Kim, J. R.; Jeong, T.-S.; Choi, S.-G.; Ryu, Y.-H.; Oh, G. T.; Baek, N.-I.; Kwon, B.-M. *Nat. Prod. Res.* **2006**, *20*, 139.
11. Sato, S.; Aoyama, C.; Takeo, J. *Bioorg. Med. Chem.* **2007**, *15*, 3445.
12. Kubo, M.; Nagai, M.; Inoue, T. *Chem. Pharm. Bull.* **1983**, *31*, 1917.
13. Furihata, K.; Seto, H. *Tetrahedron Lett.* **1999**, *40*, 6271.
14. Mohamadi, F.; Richards, N. G. J.; Guida, W. C.; Liskamp, R.; Lipton, M.; Caufield, C.; Chang, G.; Hendrickson, T.; Still, W. C. *J. Comput. Chem.* **1990**, *11*, 440.
15. Halgren, T. J. *Am. Chem. Soc.* **1990**, *112*, 4710.
16. Molecular modeling experiments employed MacroModel 9.1 equipped with the Maestro 7.5 graphical interface (Schrödinger, LLC, New York, NY, 2005) installed on a Linux Red Hat 9.0 system, and were performed using the MMFF force field.
17. All measurements were made on a Rigaku RAXIS RAPID imaging plate area detector with graphite monochromated Cu-K α radiation. *Crystal data of 2*: A colorless platelet crystal, mp 184.0–185.5 °C, C₁₉H₂₂O₃, crystal dimensions 0.15 × 0.15 × 0.12 mm, space group P-1 (#2), *a* = 7.6023 (5), *b* = 9.0220 (5), *c* = 13.1572 (8) Å, α = 71.864(4)°, β = 74.168(4)°, γ = 65.806(3)°, *V* = 771.21(8) Å³, *Z* = 2, *D*_{calc} = 1.285 g/cm³. Of the 8820 reflections that were collected, 2767 were unique (*R*_{int} = 0.041). The structure was solved by direct methods. *R*₁ = 0.0585 (*I* > 2.00 σ (*I*)). All calculations were performed using the CrystalStructure crystallographic software package except for refinement, which was performed using SHELXL-97. The refined fractional atomic coordinates, bond lengths, bond angles, and thermal parameters have been deposited at the Cambridge Crystallographic Data Centre (CCDC). CCDC 753644 contains the supplementary crystallographic data for this paper. These data can be obtained free of charge via <http://www.ccdc.cam.ac.uk/deposit>, or from the CCDC, 12 Union Road, Cambridge CB2 1EZ, UK (fax: +44 1223 336 033; e-mail: deposit@ccdc.cam.ac.uk).
18. Asakawa, Y.; Toyota, M.; Tori, M.; Hashimoto, T. *Spectroscopy* **2000**, *14*, 149; Morita, H.; Tomizawa, Y.; Tsuchiya, T.; Hirasawa, Y.; Hashimoto, T.; Asakawa, Y. *Bioorg. Med. Chem. Lett.* **2009**, *19*, 493.